PERGAMON

Global Environmental Change 9 (1999) S21–S30

GLOBAL ENVIRONMENTAL CHANGE

www.elsevier.com/locate/gloenvcha

Climate change impacts on ecosystems and the terrestrial carbon sink: a new assessment

Andrew White*, Melvin G.R. Cannell, Andrew D. Friend[1]

Institute of Terrestrial Ecology, Bush Estate, Penicuik, Midlothian EH26 0QB, UK

Received 21 May 1999

Abstract

Climate output from the UK Hadley Centre's HadCM2 and HadCM3 experiments for the period 1860 to 2100, with IS92a greenhouse gas forcing, together with predicted patterns of N deposition and increasing CO_2, were input (offline) to the dynamic vegetation model, Hybrid v4.1 (Friend et al., 1997; Friend and White, 1999). This model represents biogeochemical, biophysical and biogeographical processes, coupling the carbon, nitrogen and water cycles on a sub-daily timestep, simulating potential vegetation and transient changes in annual growth and competition between eight generalized plant types in response to climate.

Global vegetation carbon was predicted to rise from about 600 to 800 PgC (or to 650 PgC for HadCM3) while the soil carbon pool of about 1100 PgC decreased by about 8%. By the 2080s, climate change caused a partial loss of Amazonian rainforest, C_4 grasslands and temperate forest in areas of southern Europe and eastern USA, but an expansion in the boreal forest area. These changes were accompanied by a decrease in net primary productivity (NPP) of vegetation in many tropical areas, southern Europe and eastern USA (in response to warming and a decrease in rainfall), but an increase in NPP of boreal forests. Global NPP increased from 45 to 50 PgC y^{-1} in the 1990s to about 65 PgC y^{-1} in the 2080s (about 58 PgC y^{-1} for HadCM3). Global net ecosystem productivity (NEP) increased from about 1.3 PgC y^{-1} in the 1990s to about 3.6 PgC y^{-1} in the 2030s and then declined to zero by 2100 owing to a loss of carbon from declining forests in the tropics and at warm temperate latitudes — despite strengthening of the carbon sink at northern high latitudes. HadCM3 gave a more erratic temporal evolution of NEP than HadCM2, with a dramatic collapse in NEP in the 2050s.

Keywords: Carbon sink; Climate change; Elevated CO_2

1. Introduction

In Article 2 of the Framework Convention on Climate Change (FCCC), climate change is considered 'dangerous', and thus to be avoided, if it is likely to cause damage to global ecosystems. In this paper we offer a new assessment of the effects of climate change on the geographic distribution of ecosystems, their productivities and their roles as carbon sinks. Climate change which caused the disappearance or reversal of the putative terrestrial carbon sink of about 1.6 Pg y^{-1} (Houghton et al., 1998) would of itself constitute a dangerous positive feedback to the climate system, so we pay special attention to changes in the amount of carbon stored in global vegetation and soils.

It is only in the last few years that it has been possible to estimate the impact of climate change on ecosystems in a reliable and meaningful way. First, it required the development of 'dynamic global vegetation models' (DGVMs) which couple plant–soil carbon, N and water cycles, which include atmosphere–vegetation interactions and represent competitive processes that determine transient shifts in vegetation types and properties (Hurtt et al., 1998). Hybrid v4.1 is one of a few DGVMs which fulfils those requirements (Friend et al., 1997; Cramer et al., 1999). Second, it required transient output from GCMs, which has only recently become available (Xiao et al., 1998; Foley et al., 1998). And thirdly, it has been increasingly apparent that consideration has to be given to the controversial role of atmospheric N deposition (Hudson et al., 1994; Townsend et al., 1996; Holland et al., 1997; Nadelhoffer et al., 1999).

* Corresponding author. Current address: Department of Mathematics, Heriot-Watt University, Edinburgh EH14 4AS, UK.

E-mail address: awhite@ite.ac.uk (A. White)

[1] Andrew Friend is currently located at the NASA-GISS in New York.

0959-3780/99/$ - see front matter
PII: S0959-3780(99)00016-3

This re-assessment meets these three requirements. However, effects of land use change and fire are ignored and Hybrid does not represent dispersal processes. Thus, the impacts reported here refer to potential vegetation, in the absence of disturbance and assuming that all vegetation types are available to grow wherever and whenever the climate permits.

2. Overview of the dynamic global vegetation model, hybrid v4.1

A complete description of the Hybrid model is given by Friend et al. (1997) and Friend and White (1999) who evaluated its ability to simulate measured carbon fluxes at particular sites and the pre-industrial global distribution of vegetation types, NPP and carbon. Here, we outline the essential properties of the model.

The model operates conceptually like a forest gap model, in which individuals of all potential plant types are seeded every year (i.e. there are no dispersal constraint) into 200 m^2 plots and can grow, die and regenerate year by year, with all underlying processes calculated on a sub-daily timestep. Vegetation types are assigned different parameter values which determine their success in competing for light, water and N in any climatic regime and hence the resulting vegetation. Thus, the model describes the transient responses and properties of vegetation, which can be composed of different proportions of specified plant types at any time. However, unlike most gap models, plant growth is determined entirely by climatic variables operating through plant physiological and soil processes. The carbon, water and nutrient cycles are coupled, including all the major interactions, feedbacks and exchanges between the soil, vegetation and atmosphere. The model contains no statistical relationships between vegetation properties and the current climate except for phenology.

2.1. Plant and vegetation types

The model is parameterised for three main classes of vegetation: herbaceous, broadleaved trees and needleleaved trees (Table 1), which are given different values of up to 16 parameters (Table 2). These main classes are then divided into eight generalised plant types, as shown in Table 1, by distinguishing C_3 and C_4 herbaceous plants, evergreen and deciduous trees and cold and dry deciduous trees. C_3 and C_4 herbaceous plants have different photosynthesis submodels; cold deciduous trees shed their leaves in response to daylength and refoliate in response to a degree-day requirement; dry deciduous trees shed their leaves when the soil water potential falls below -1.49 MPa (10^6 Pa) and refoliate when it rises above -0.5 MPa. The eight generalised plant types were then used to define seven vegetation types, based on the proportion of biomass present in the generalised plant types (Table 1).

2.2. Key processes represented

The canopy is divided into 1 m layers and attenuation down the canopy of photosynthetically active and short wave radiation is calculated using Beer's law with defined extinction and reflection coefficients (Table 2, 1–4). Canopy photosynthesis is linearly related to the photosynthetic rate of the uppermost leaves. The vertical profile of N in the canopy is optimized to the time-mean profile of PAR.

C_3 and C_4 photosynthesis are calculated using a biochemical approach based on Farquhar and von Caemmerer (1982) and Collatz et al. (1991), respectively. The three main classes differ in the fraction of foliage N not used in Rubisco or thylakoids (Table 2, 5). Stomatal conductance is calculated using empirical relationships between stomatal conductance and irradiance, soil water potential, air temperature, above-canopy water vapour pressure deficit and above-canopy $[CO_2]$ (Jarvis, 1976; adapted by Stewart, 1988; see also, Friend, 1995). The main classes differ in the ratio between maximal stomatal conductance and Rubisco N (Table 2, 6). Foliage and fine root maintenance respiration rates are linear functions of N content; sapwood maintenance respiration is a linear function of living sapwood biomass. Herbaceous respiration rates are linear functions of biomass. All respiration components are exponential functions of air temperature.

Table 1
Vegetation types defined in this study, showing their relationship to eight generalised plant types in Hybrid v4.1 (defined by C_3 or C_4 photosynthesis and phenology) and three main classes (defined by the parameters given in Table 2)

Main classes	Herbaceous	Broadleaved tree	Needleleaved tree
Generalized plant types	(1) C4 photosynthesis (2) C3 photosynthesis	(3) Evergreen (4) Cold deciduous (5) Dry deciduous	(6) Dry deciduous (7) Cold deciduous (8) Evergreen
Vegetation types	(i) C4 grassland (ii) C3 grassland (iii) savanna–steppe-tundra (herbaceous biomass > 10% of tree biomass)	(iv) broadleaf evergreen (v) broadleaf cold deciduous	(vi) coniferous forest (90–100% biomass is 7 or 8) (vii) mixed forest (v and vi, with neither more than 90% of the biomass)

Table 2
Parameters used to define the three main classes of plants in Hybrid v4.1 (Friend et al., 1997)

Parameter	Herbaceous	Broadleaf tree	Needleleaf tree	Units
1. Shortwave irradiance extinction coefficient	0.48	0.48	0.48	dimensionless
2. Shortwave irradiance reflection coefficient	0.20	0.20	0.11	fraction
3. Photosynthetically active irradiance extinction coefficient	0.65	0.65	0.50	dimensionless
4. Photosynthetically active irradiance reflection coefficient	0.05	0.05	0.03	fraction
5. Fraction of foliage N not used in Rubisco or thylakoids	0.67	0.67	0.83	fraction
6. Ratio between max. stomatal conductance and Rubisco nitrogen	1359	1670	2220	mol(H_2O) m^{-2} s^{-1}/(kg (RubiscoN) m^{-2})
7. Ratio of bark thickness to *D* (diameter)	—	0.033	0.03	m m^{-1}
8. Tree form factor (used for calculating woody carbon mass)	—	0.60	0.56	dimensionless
9. Allometry coefficient for *H* (height) from *D* (diameter)	—	28.51	32.95	m^{-1}
10. Allometry exponent for *H* (height) from *D* (diameter)	—	0.467	0.588	dimensionless
11. Fraction of wood plus bark below ground	—	0.220	0.222	fraction
12. Mean wood plus bark density	—	305	205	kg C m^{-3}
13. Maximum foliage to sapwood area ratio	—	4170	3330	m^2 m^{-2}
14. Fraction of sapwood alive	—	0.1700	0.0708	fraction
15. Specific leaf area	36	36	12	m^2 kg C^{-1}
16. Turnover rate of foliage	1.13	1.00	0.33	fraction y^{-1}

Trees are assigned initial diameters, which then determine the leaf area index and biomass of tree parts according to allometric relationships (Shinozaki et al., 1964; Friend et al., 1997). Wood cross-sectional area at breast height is calculated assuming a ratio of diameter at breast height to bark thickness (Table 2, 7). Woody biomass is then calculated using a form factor (Table 2, 8), calculated tree height (Table 2, 9 and 10), a proportion of woody biomass below ground (Table 2, 11) and wood specific gravity (Table 2, 12). There are also defined values for ratio of foliage to sapwood area, fraction of live sapwood, specific leaf area and turnover rate of foliage (Table 2, 13–16).

N uptake is a function of fine root biomass, plant C : N ratio, soil surface temperature and soil mineral N, which includes N biologically fixed and deposited from the atmosphere. Trees have access to all mineral N, whereas the herbaceous layer has access to only a fraction, given by the ratio of the soil water holding capacity of the top two hydrological layers over the total capacity for all three layers.

For trees, the maximum possible foliage and fine root C and N contents are calculated at the beginning of the year. During the year, litter C and N are lost from these components (different tree species are assumed to have the same fine root turnover but different foliage turnover rates, Table 2), and if sufficient storage is available they are restored to their maximum values. If the lowest 1m of the crown experiences a negative C balance then the maximum foliage area in the next year is given by the amount of foliage displayed above the lowest layer and the height to the base of the crown is increased by 1m. Also, since the foliage to sapwood area is fixed, when trees experience a negative C balance at the base of their crowns some sapwood will be converted to heartwood. A fixed ratio between foliage mass and fine root mass, and a fixed fraction of woody tissue below ground are also assumed (Friend et al., 1997).

For herbs and grasses, C and N litter production is calculated as a fixed fraction of the foliage, structural and fine root compartments. Allocation of C is parameterised to maintain fixed ratios between these compartments. If the lowest 10% of foliage has a net negative C balance on the previous day, then the new foliage area is limited to a maximum of 90% of its previous value. Any C remaining after allocation is added to a storage pool. N is allocated to maintain fixed relative C : N ratios between the three tissue compartments.

The daytime energy balance of the canopy is solved to calculate the rate of transpiration and foliage temperature. Interception loss is calculated. The soil C and N dynamics model is based on Century (Parton et al., 1993) as formulated by Comins and McMurtrie (1993). The soil is divided into three layers: 0–5 cm, 5–20 cm and 20–100 cm depth. Herbaceous vegetation has access to water and N in the top two layers, whereas trees can access all layers. The total soil water holding capacity is determined from soil carbon. A soil temperature profile is used to calculate the depth of frozen soil, with all water below this depth assumed frozen, and therefore unavailable and forming an increased resistance to drainage (Wang and Polglase, 1995; White et al., 1999).

3. Simulations

The Hybrid model was spun up for 500 yrs to reach a near-steady-state in the 1860 climate (Friend and White, 1999). It was then run to 2100 in transient simulations with ten independent 200 m^2 plots in each GCM grid square, driven by transient climate output from the Hadley Centre coupled atmosphere-ocean GCM. The use of ten plots has previously been shown to be sufficient to obtain a reliable estimate of mean ecosystem behaviour (Friend et al., 1997, Friend and White, 1999). The output from four HadCM2 simulations was compared with output from one HadCM3 simulation (see Hulme et al., 1999). All climate simulations were based on an IS92a-type scenario of greenhouse gas forcing, excluding sulphate aerosols.

Predicted climate anomalies were considered to be more reliable than absolute model climate predictions as it partially removes climate model biases from predictions of the present day vegetation distribution. Consequently, GCM anomalies of temperature, diurnal temperature range, relative humidity, downward shortwave radiation and precipitation were calculated as mean decadal monthly differences relative to the 1970s. These anomalies were then added to a global observational climatology (Hulme et al., 1999). Daily and sub-daily values of the climate variables were then derived using a stochastic weather generator parameterized for each decade using mean monthly values of these climate variables (Richardson and Wright, 1984; Friend, 1998).

Atmospheric CO_2 concentrations were increased according to the GCM forcing scenario, rising from 280 ppm in 1860 to nearly 800 ppm in 2100 (see Table 1, Hulme et al. (1999) for mean values at three time slices which highlight the difference in forcing between the HadCM2 and HadCM3 simulations). Biological N fixation was assumed to be 10 kgN ha^{-1} y^{-1}. Atmospheric N deposition for each grid cell was derived from NH_x and NO_y deposition estimates for pre-industrial, current and 2050 conditions, assuming an exponential increase with time (Holland et al., 1997; Dentener, pers comm.).

4. Global carbon stocks

Present-day vegetation was predicted to contain 600–630 PgC and soils 1080–1160 PgC, depending on the GCM experiment (Fig. 1). These predictions may be compared with global inventory estimates of 420–830 PgC in vegetation and 1200–1600 PgC in soils (Post et al., 1990). The low model estimate for soil carbon may be attributed to the use of the same decay constants and temperature response functions for decomposition at all latitudes (Friend and White, 1999).

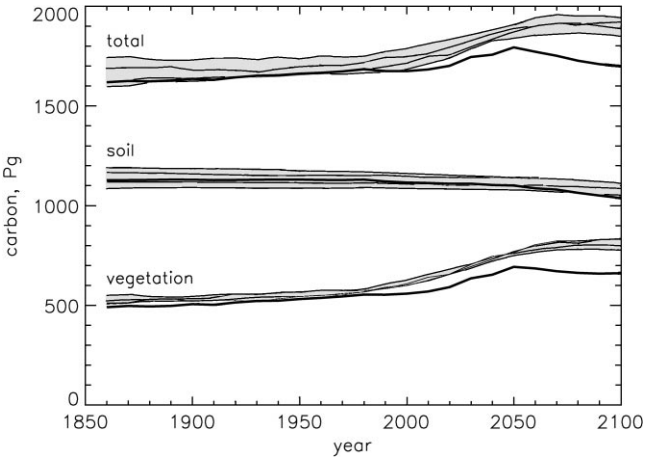

Fig. 1. Global stocks of carbon in vegetation and soil, predicted by Hybrid in response to climate output from four individual simulations of HadCM2 (thin solid lines) and one HadCM3 simulation (thick solid line). The grey shading covers the range of the HadCM2 individual simulations.

In the HadCM2-driven simulations, vegetation carbon was predicted to increase by 290 PgC or 56% between 1860 and 2100. Total carbon increased less (by 238 PgC, or 14% between 1860 and 2100) because soils lost 52 PgC or 5% during the simulation (Fig. 1). In the HadCM3-driven simulation, the vegetation accumulated less carbon (170 PgC or 35% between 1860 and 2100), the soil lost more (90 PgC or 8%) and total carbon was predicted to peak in the 2050s with only an 80 PgC or 5% increase in total carbon over the simulation period.

5. Geographic distribution of vegetation types

Hybrid successfully predicted the current broad geographic distribution of potential vegetation types (Friend and White, 1999). The shifts in vegetation distribution in response to climate change were qualitatively similar in the HadCM2- and HadCM3-driven simulations, but were markedly more severe in the HadCM3 climate (Fig. 2), owing to greater warming and rainfall anomalies, especially in parts of the tropics (Hulme et al., 1999). Four key changes were predicted.

5.1. Loss of Amazonian rainforest

In all simulations, some areas of tropical evergreen forest in Amazonia were predicted to change to savanna, grassland or even desert by the 2080s, in response to warming of over 7°C and decreases in rainfall of up to 500 mm y^{-1}. HadCM3 predicted larger and more widespread temperature and rainfall anomalies in this region than any HadCM2 simulation so resulted in the loss of larger areas of forest (Fig. 2).

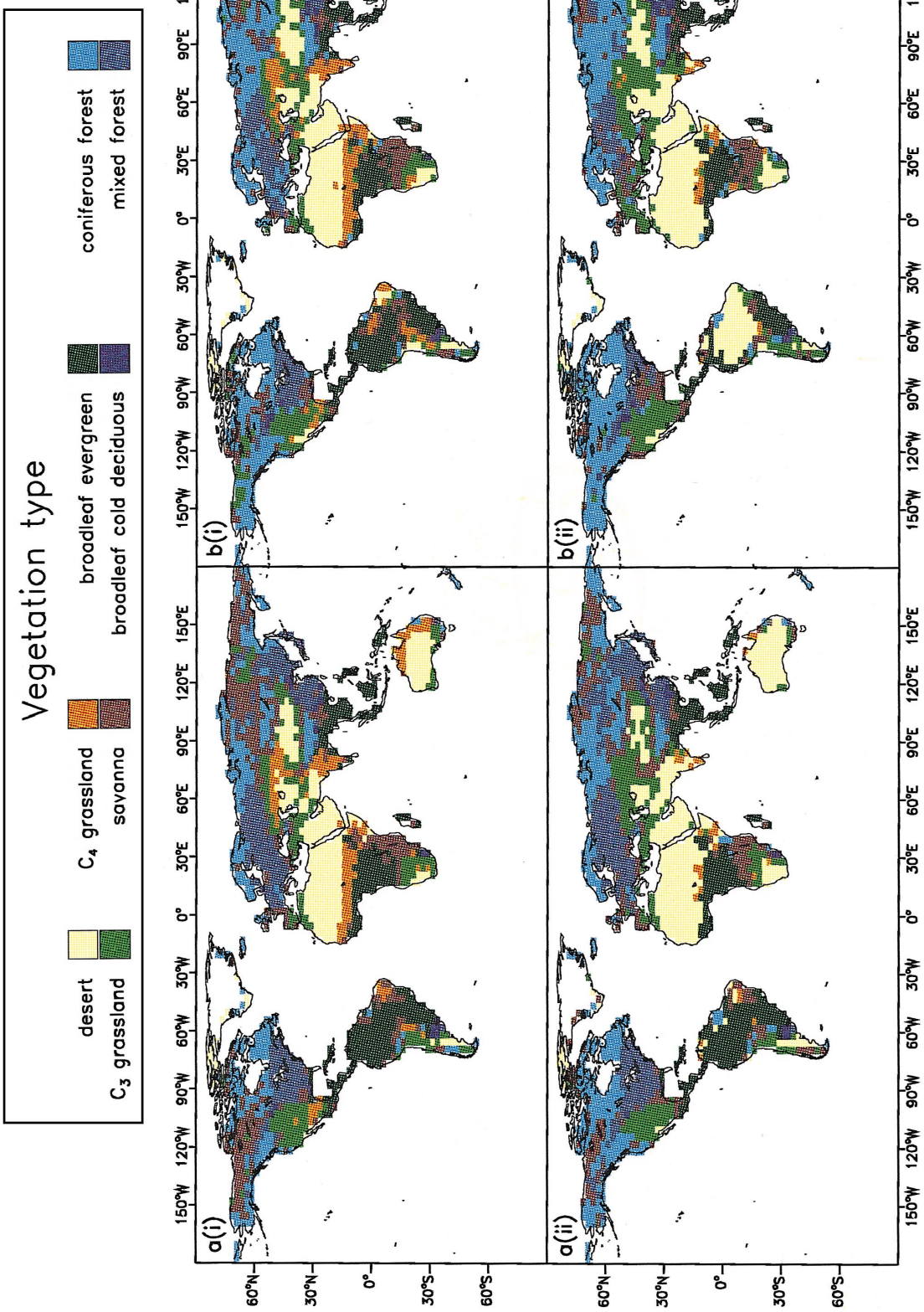

Fig. 2. Distribution of seven vegetation types, plus desert, predicted for (a) the average output of four Hybrid runs when driven by each of the HadCM2 simulations and (b) Hybrid driven by the HadCM3 simulation, in (i) the 1990s and (ii) the 2080s.

5.2. Loss of C_4 tropical grasslands

In all simulations, large areas of tropical C_4 grasslands (e.g. in the Sahel, India and Australia) were lost to desert by the 2080s in response to warming, increasing CO_2 and decreased rainfall, or superceded by C_3 grasslands where rainfall increased (Fig. 2).

5.3. Loss of temperate forests

In the HadCM3-driven simulation, annual precipitation decreases of up to 200 mm y^{-1} resulted in the conversion of large areas of temperate forest to grassland or savanna in southern Europe and eastern USA. Precipitation anomalies were not large enough in the HadCM2 simulations to bring about any large loss of temperate forests (Fig. 2).

5.4. Expansion of boreal forests

In all simulations, needleleaved boreal forest extended northwards in response to warming, with a loss of tundra (see also White et al., 1999) and southwards in Asia in response to increased precipitation.

6. Global net primary productivity

Present-day global NPP was predicted to be in the range 46.6–49.5 PgC y^{-1} (Fig. 3) at the low end of the range estimated by others (48.3–67.6 PgC y^{-1}; Field et al., 1998; 44.4–66.3 PgC y^{-1}; Cramer et al., 1999). Low predicted NPP values could be attributed to somewhat low values of short-wave radiation, which were derived from cloud cover in the global observational climatology (Hulme et al., 1999). Over the period 1860–2100, global NPP increased by 23.3 PgC y^{-1} or 56% in the HadCM2 driven simulations and by 17.5 PgC y^{-1} or 43% in the HadCM3-driven simulation (Fig. 3). For the HadCM3 climate, NPP did not increase consistently after the 2020s. It may be noted that the shapes of the NPP curves in Fig. 3 are similar to those for vegetation carbon in Fig. 1.

The pre-industrial geographic distribution of NPP was simulated reasonably successfully (Fig. 4; Friend and White, 1999). Over the period 1990-2080, the NPP of northern forests increased markedly in response to warming, increased CO_2 and, in some areas, increased precipitation. By contrast, NPP decreased in southern Europe, eastern USA and in many areas of the tropics (Fig. 4). Areas with a large drop in NPP corresponded to areas where forests declined and were transformed to savanna, grassland or desert (Fig. 2). It should be noted that the HadCM3 simulation predicted anomalously low rainfall and high temperatures in Amazonia in the 1990s, giving rise to low NPPs, so that the decrease in NPP between the 1990s the 2080s was anomalously small, although the forest was replaced by grassland or desert over this period.

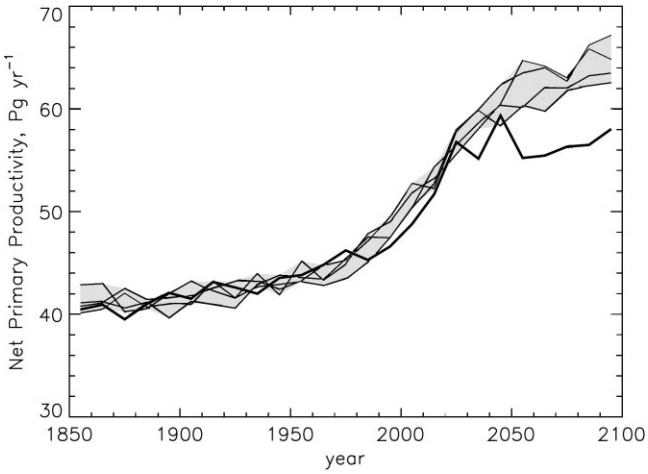

Fig. 3. Global annual net primary productivity (NPP), predicted by Hybrid in response to climate output from four individual simulations of HadCM2 (thin solid lines) and one HadCM3 simulation (thick solid line). The grey shading covers the range of the HadCM2 individual simulation.

7. Global net ecosystem productivity

NEP is the difference between NPP and heterotrophic (soil) respiration — the rate of change of stored carbon or net flux of carbon between the land and atmosphere.

In the HadCM2-driven simulations, NEP increased after about 1970 to 0.6–1.8 PgC y^{-1} in the 1990s, to 2.5–4.5 PgC y^{-1} in the 2030s and then fell to below zero by 2100 (Fig. 5). Thus, Hybrid predicted a growing terrestrial carbon sink, roughly in line with inventory and deconvolution estimates (Houghton et al., 1998) but a collapse and reversal of this sink during the next century. The HadCM3-driven simulation predicted an anomalous drop in NEP in the 1980–1990s, caused by low rainfall and warming in parts of the tropics, and a much more dramatic drop in NEP in the 2050s than occurred in HadCM2 driven simulations. In all cases, decreases in NEP were associated with the decline or death of areas of tropical and/or temperate forests, as stated above (Fig. 2).

The latitudinally resolved predictions of NEP show where the carbon sinks and sources were located over time (Fig. 6). The HadCM2-driven simulations predicted that the current sink is located at 30–60°N and 0–15°S, that is, in both the northern and tropical forests. The northern sink strengthened throughout the simulation, whereas the tropical sink peaked in the 2030s and became increasingly negative after the 2050s. The HadCM3-driven simulation predicted that the northern

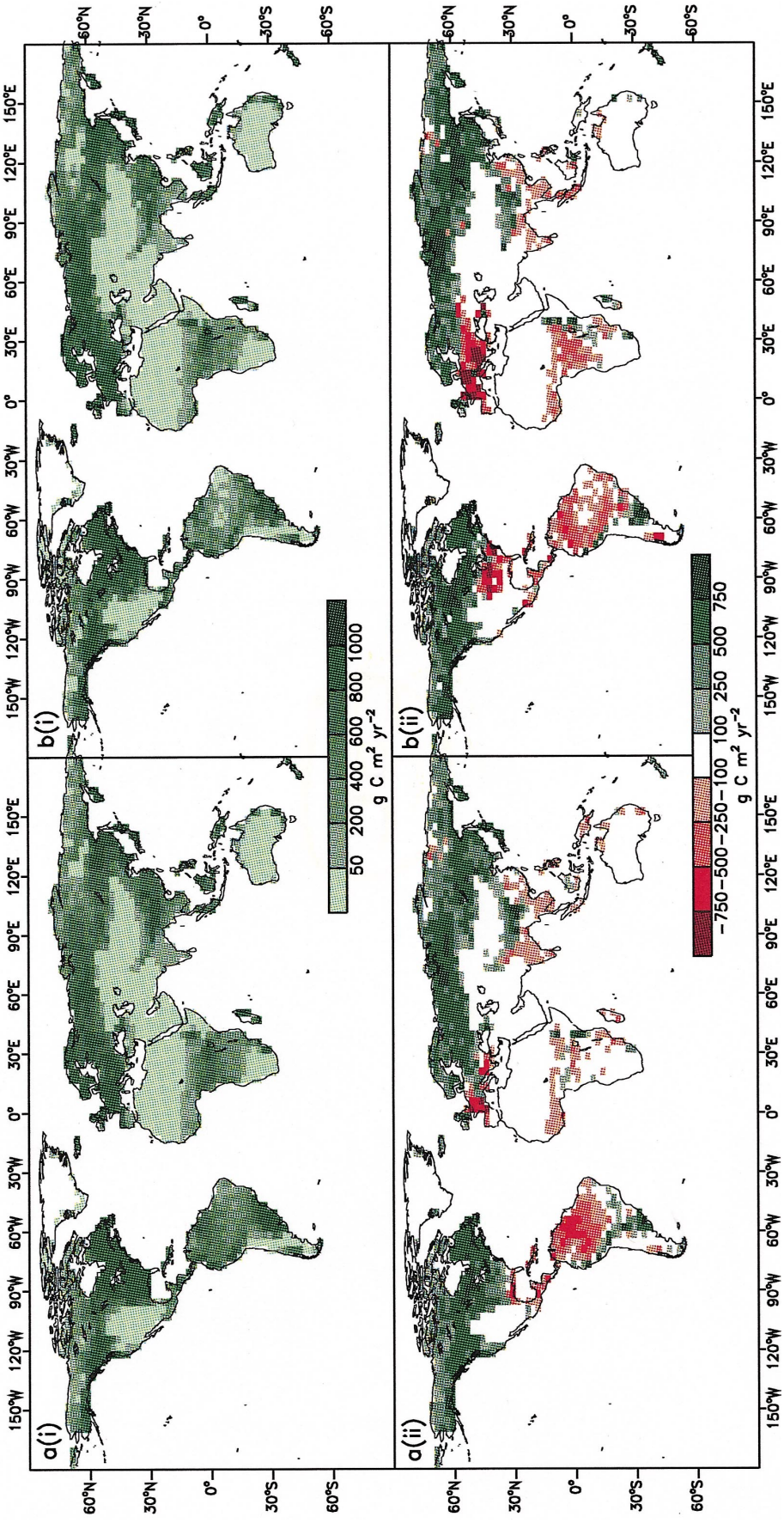

Fig. 4. Net primary productivity (NPP) of vegetation predicted for (a) the average output of four Hybrid runs when driven by each of the HadCM2 simulations and (b) Hybrid driven by the HadCM3 simulation, in (i) the 1990s and (ii) the 2080s minus the 1990s (i.e. the change in NPP between these periods).

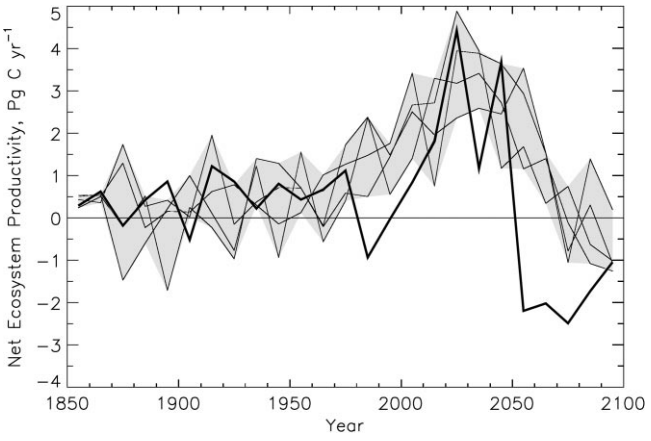

Fig. 5. Global annual net ecosystem productivity (NEP), predicted by Hybrid in response to climate output from four individual simulations of HadCM2 (thin solid lines) and one HadCM3 simulation (thick solid line). The grey shading covers the range of the HadCM2 individual simulations.

sink would be restricted to the boreal forest region after the 2050s and that both the temperate and tropical forests would be carbon sources during the latter half of the next century. Fig. 6 clearly shows the anomalous period of hot, dry conditions predicted by HadCM3 in parts of the tropics in the 1980–2000 period, causing a decline in forest biomass (although not tree death) and a temporary carbon source.

8. Discussion

This study used a combined biogeochemical, biophysical and biogeographical ecosystem model (Hybrid v4.1) with realistic transient behaviour (as in gap models) driven by transient HadCM2 and HadCM3 climate predictions, with an IS92a-type forcing scenario (excluding aerosol forcing), to predict the effects of climate change on terrestrial ecosystems and the terrestrial carbon sink. The climate predictions were combined with predictions of N deposition and increasing atmospheric CO_2. Confidence in the predictions of the ecosystem model may be derived from the fact that it successfully predicted the geographic distribution of broad vegetation types, their NPPs and carbon contents, within measured ranges (Friend and White, 1999). Moreover, the model predicted the development and current existence of a terrestrial carbon sink of 0.6–1.8 PgC y^{-1}, which is within the range estimated by other methods (Houghton et al., 1998). Further confidence in the ability of the model to predict ecosystem responses to climate, increasing CO_2 and N deposition has to be derived from the ways in which individual plant and soil processes are represented and coupled (Friend et al., 1997). The major limitations of the model are that it does not include land use changes — it simulates only potential vegetation. Also, of course, it is not coupled to the GCM, so that vegetation-climate feedbacks involving energy, water and carbon are not included.

Overall, the findings suggest that climate change, combined with increasing CO_2 and N deposition, will have a beneficial or benign effect on most ecosystems until about the 2050s. But thereafter, shifts in temperature and precipitation become large enough to adversely affect the growth of many tropical and temperate forests, with a decrease in NPP followed by forest decline and a loss of carbon from vegetation and soils.

In the model, the early beneficial effects of climate change were due mainly to the increase in atmospheric CO_2, combined with warming, which increased canopy photosynthesis and water use efficiency in accordance with plant physiological relations, increasing NPP, forest biomass (increasing vegetation carbon), litterfall and potentially soil carbon. In many regions, N deposition amplified the CO_2-fertilization effect to a moderate extent (Nadelhoffer et al., 1999) and the increase in NPP and forest biomass was not highly constrained by N supply because of an increase in foliar C : N ratio and enhanced N mineralization in response to soil warming. In these respects the model performed similarly to others which include N dynamics (Foley et al., 1996; Kellomaki and Vaisanen, 1997; Xiao et al., 1998). The effect of increasing CO_2 obviously diminished as photosynthesis saturated, but even so, at high northern latitudes the model predicted a continuing beneficial effect of climate change on NPP and NEP (despite accelerated soil respiration) until at least 2100 (see White et al., 1999).

After the 2050s, the warming and shifts in rainfall predicted by HadCM2, and especially the HadCM3, simulations became large enough to reach critical levels in some tropical and temperate regions. Increases in photorespiration, maintenance respiration and saturation deficits — causing stomatal closure — lowered forest NPP and initiated forest decline in some tropical and temperate forest regions. By the 2080s, the climate could not support forest vegetation in many former forest areas and the loss of carbon from declining forests effectively eliminated the global terrestrial carbon sink. Both of these potential changes are clearly 'dangerous' in terms of Article 2 of the FCCC. The declines in NPP and biomass in parts of the tropics imply a loss of productivity of fuelwood and perhaps of non-grain crops, whose yield is related to annual biomass production (e.g. cassava, banana and potato). The predicted loss of forests in Amazonia and southern Europe has major socio-economic and environmental implications and the loss of the terrestrial carbon sink implies an accelerated increase in greenhouse gas concentrations.

It should be stressed that the predictions of forest and terrestrial carbon loss are not specific to the Hybrid model. Most dynamic vegetation models would have difficulty in sustaining forests in tropical or temperate

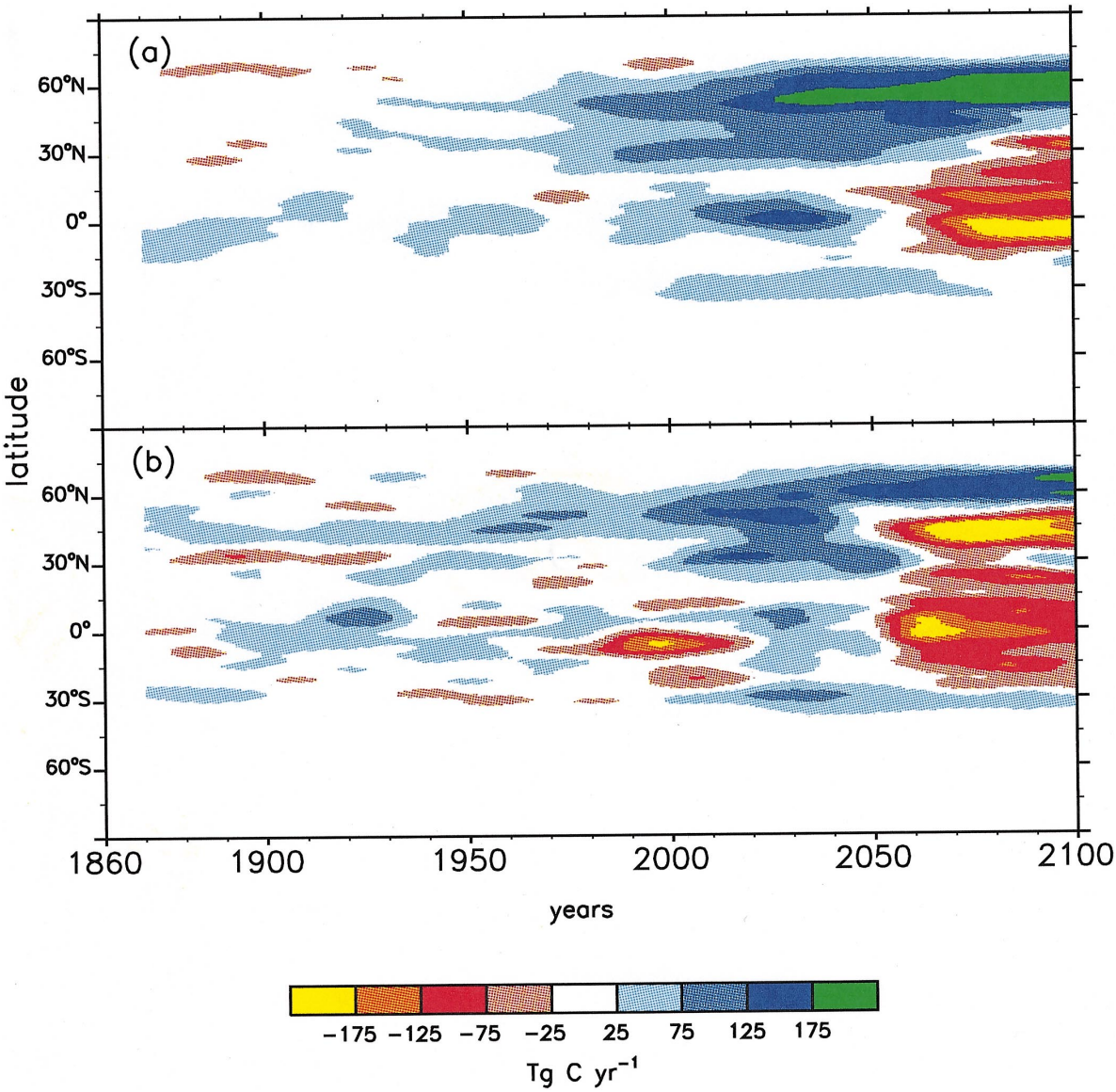

Fig. 6. Predicted annual net ecosystem productivity (NEP) resolved by latitude, for (a) the average output of four Hybrid runs when driven by each of the HadCM2 simulations and (b) Hybrid driven by the HadCM3 simulation.

regions subject to temperature increases of up to 7°C and/or decreases in rainfall of over 400 mm y^{-1}. However, models which do not simulate transient changes in vegetation composition and distribution, or couple the carbon and N cycles, are not able to quantify the transient carbon loss the accompanies forest decline and so do not predict a marked decline on the terrestrial carbon sink (Cao and Woodward, 1998).

The salient findings of this study are a consequence of the extreme climate predicted by the Hadley Centre GCM. The difference between the HadCM2 and HadCM3 simulations is a measure of one model-related source of uncertainty in climate predictions. Nevertheless, this study suggests that climate change predicted by the HadCM2 and HadCM3 simulations when forced by a 1% per annum growth in greenhouse gas concentrations presents a future that could potentially damage many natural ecosystems.

Acknowledgements

This work was supported by the UK Department of the Environment, Transport and the Regions under contract EPG 1/1/64.

References

Cao, M., Woodward, F.I., 1998. Dynamic responses of terrestrial ecosystem carbon cycling to global climate change. Nature 393, 249–252.

Collatz, G.J., Ball, J.T., Grivet, C., Berry, J.A., 1991. Physiological and environmental regulation of stomatal conductance, photosynthesis and transpiration: a model that includes a laminar boundary layer. Agricultural and Forest Meteorology 54, 107–136.

Comins, H.N., McMurtrie, R.E., 1993. Long-term response of nutrient-limited forests to CO_2 enrichment. Ecological Applications 3, 666–682.

Cramer, W., Kicklighter, D.W., Bondeau, A., Moore III, B., Churkina, G., Nemry, B., Ruimy, A., Schloss, A.L., the participants in the Potsdam NPP model intercomparison, 1999. Comparing global models of terrestrial net primary productivity (NPP): overview and key results. Global Change Biology 5, 1–15.

Farquhar, G.D., von Caemmerer, S., 1982. Modelling of photosynthetic response to environmental conditions. In: Lange, O., Nobel, P., Osmond, C., Zieger, H. (Eds.), Physiological Plant Ecology II: Water Relations and Carbon Assimilation. Springer, Berlin.

Field, C.B., Behrenfeld, M.J., Randerson, J.T., Falkowski, P., 1998. Primary production of the biosphere: Integrating terrestrial and oceanic components. Science 281, 237–240.

Foley, J.A., Levis, S., Prentice, I.C., Pollard, D., Thompson, S.L., 1998. Coupling dynamic models of climate and vegetation. Global Change Biology 4, 561–579.

Friend, A.D., 1995. PGEN: an integrated model of leaf photosynthesis, transpiration and conductance. Ecological Modelling 77, 233–255.

Friend, A.D., 1998. Parameterisation of a global daily weather generator for terrestrial ecosystem modelling. Ecological Modelling 109, 121–149.

Friend, A.D., Stevens, A.K., Knox, R.G., Cannell, M.G.R., 1997. A process-based terrestrial biosphere model of ecosystem dynamics (Hybrid v3.0). Ecological Modelling 95, 249–287.

Friend, A.D., White, A., 1999. Evaluation and analysis of a dynamic terrestrial ecosystem model under pre-industrial conditions at the global scale. Global Biogeochemical Cycles. (in press).

Holland, E.A., Braswell, B.H., Lamarque, J.F., Townsend, A., Sulzman, J., Muller, J.F., Dentener, F., Brasseur, G., Levy, H., Penner, J.E., Roelofs, G.J., 1997. Variations in the predicted spatial distribution of atmospheric nitrogen deposition and their impact on carbon uptake by terrestrial ecosystems. Journal of Geophysical Research 102, 15 849–15 866.

Houghton, R.A., Davidson, E.A., Woodwell, G.M., 1998. Missing sinks, feedbacks and understanding the role of terrestrial ecosystems in the global carbon balance. Global Biogeochemical Cycles 12, 25–34.

Hudson, R.J.M., Gherini, S.A., Goldstein, R.A., 1994. Modeling the global carbon cycle: nitrogen fertilization of the terrestrial biosphere and the 'missing' sink. Global Biogeochemical Cycles 8, 307–333.

Hulme, M., Mitchell, J., Ingram, M., Johns, T., New, M., Viner, D., 1999. Climate change scenarios for global impacts studies. Global Environmental Change 9, S3–S19.

Hurtt, G., Moorcroft, P.R., Pacala, S.W., Levin, S.A., 1998. Terrestrial models and global change: challenges for the future. Global Change Biology 4, 581–590.

Jarvis, P.G., 1976. The interpretation of the variations in leaf water potential and stomatal conductance found in canopies in the field. Philosophical Transactions of the Royal Society of London. Series B 273, 593–610.

Kellomaki, S., Vaisanen, H., 1997. Modelling the dynamics of the forest ecosystem for climate change studies in the boreal conditions. Ecological Modelling 97, 121–140.

Nadelhoffer, K.J., Emmett, B.A., Gunderson, P., Janne Kjonaas, O., Koopmans, C.J., Schleppi, P., Tietema, A., Wright, R.F., 1999. Nitrogen deposition makes a minor contribution to carbon sequestration in temperate forests. Nature 398, 145–147.

Parton, W.J., Scurlock, J.M.O., Ojima, D.S., Gilmanov, T.G., Scholes, R.J., Schimel, D.S., Kirchner, T., Menaut, J.C., Seastedt, T., Moya, E.G., Kamnalrut, A., Kinyamrio, J.I., 1993. Observations and modelling of biomass and soil organic matter dynamics for the grassland biome worldwide. Global Biogeochemical Cycles 7, 785–809.

Post, W.M., Peng, T.H., Emmanuel, W.R., King, A.W., Dale, V.H., De Angelis, D.L., 1990. The global carbon cycle. American Scientist 78, 310–326.

Richardson, C.W., Wright, D.A. 1984. WGEN: A Model for Generating Daily Weather Variables, U. S. Department of Agriculture, Agricultural Research Service.

Shinozaki, K., Yoda, K., Hozumi, K., Kira, T., 1964. A quantitative analysis of plant form – the pipe model theory. I. Basic analysis. Japanese Journal of Ecology 14, 97–105.

Stewart, J.B., 1988. Modelling surface conductance of pine forest. Agricultural and Forest Meteorology 43, 19–35.

Townsend, A.R., Braswell, B.H., Holland, E.A., Penner, J.E., 1996. Spatial and temporal patterns in terrestrial carbon storage due to deposition of fossil fuel nitrogen. Ecological Applications 6, 806–814.

Wang, Y.P., Polglase, P.J., 1995. Carbon balance in the tundra, boreal forest and humid tropical forest during climate change: scaling up from leaf physiology and soil carbon dynamics. Plant, Cell and Environment 18, 1226–1244.

White, A., Cannell, M.G.R., Friend, A.D., 1999. The high-latitude terrestrial carbon sink: a model analysis. Global Change Biology, in press.

Xiao, X., Melillo, J.M., Kicklighter, D.W., McGuire, A.D., Prinn, R.G., Wang, C., Stone, P.H., Sokolov, A., 1998. Transient climate change and net ecosystem production of the terrestrial biosphere. Global Biogeochemical Cycles 12, 345–360.